J Nanopart Res (2014) 16:2243
DOI 10.1007/s11051-014-2243-3

RESEARCH PAPER

Influence of silver nanoparticles on the activity of rat liver mitochondrial ATPase

Mariela Chichova · Milena Shkodrova · Penka Vasileva · Katerina Kirilova · Diliana Doncheva-Stoimenova

Received: 17 July 2013 / Accepted: 2 January 2014 / Published online: 16 January 2014

Abstract Mitochondria are one of the most sensitive targets for the toxicity of silver nanoparticles (AgNPs). Limited studies have demonstrated nanoparticle-induced impairment of mitochondrial oxidative phosphorylation. Reduced adenosine triphosphate (ATP) production can be due to inhibition of the respiratory chain and/or to direct effects of AgNPs on the activity of mitochondrial ATP synthase/ATPase. In this regard, we synthesized and evaluated the in vitro effects of two types of AgNPs with various environmental friendly coatings—polysaccharide starch (AgNPs/Starch, $D_{av} = 15.4 \pm 3.9$ nm) and trisaccharide raffinose (AgNPs/Raff, $D_{av} = 24.8 \pm 6.8$ nm), with an emphasis on their potential action on rat liver mitochondrial ATPase. Both types of AgNPs showed decoupling effect on intact mitochondria. Unlike AgNPs/Raff, AgNPs/Starch reduced 2,4-dinitrophenol-stimulated ATPase activity of intact mitochondria, which suggests that they are able to penetrate the inner mitochondrial membrane. Both types of AgNPs inhibited ATPase activity of freeze/thawed mitochondria and submitochondrial particles as the effects of AgNPs/Starch were more pronounced. UV–Visible absorption measurements showed changes in the absorption spectrum of AgNPs/Raff added to the reaction medium. This suggests nanoparticle aggregation and thus a possible reduction in their reactivity. The distinction in the effects of the two types AgNPs studied may be due to their different sizes and/or to the stabilizing agents used for their synthesis, which determine AgNPs colloidal stability in the assay media. This study suggests the need for further research into the importance of surface modifications of AgNPs for their interaction with cellular components. Our findings could contribute to the elucidation of the mechanisms underlying AgNPs toxicity.

Keywords Silver nanoparticles · Carbohydrate stabilizing agents · Mitochondria · Mitochondrial ATPase · Bioenergetics · Health effects

Electronic supplementary material The online version of this article (doi:10.1007/s11051-014-2243-3) contains supplementary material, which is available to authorized users.

M. Chichova (✉) · M. Shkodrova · K. Kirilova · D. Doncheva-Stoimenova
Department of Animal and Human Physiology, Faculty of Biology, Sofia University "St. Kliment Ohridski", Dragan Tzankov Blvd. 8, 1164 Sofia, Bulgaria
e-mail: marielach@biofac.uni-sofia.bg

P. Vasileva
Laboratory of Nanoparticle Science and Technology, Department of General and Inorganic Chemistry, Faculty of Chemistry and Pharmacy, Sofia University "St. Kliment Ohridski", James Bourchier Blvd. 1, 1164 Sofia, Bulgaria

Introduction

Nanomaterials are increasingly being used for commercial purposes because of their unique physicochemical properties. At the same time, concerns about

their adverse effects on human health and the environment are growing. It is estimated that of all nanoparticles used in consumer products, the silver nanoparticles (AgNPs) currently have the highest degree of commercialization (Woodrow Wilson International Center for Scholars 2013) with a wide range of industrial and medical applications that may put human health at risk. Following their entry into systemic circulation, AgNPs may migrate to liver, spleen, lungs, kidneys, and brain and induce toxicity (Rahman et al. 2009; Tang et al. 2009). Interactions between AgNPs and living system are not as yet fully understood. In vitro studies suggest that the mechanisms of AgNPs cytotoxicity include apoptosis, inflammation, free radical production, membrane damage, and cell death (AshaRani et al. 2009; Eom and Choi 2010).

Mitochondria play a key role in cell physiology, producing energy, and participating in number of processes such as production of reactive oxygen species (Turrens 2003), organization of cell apoptosis (Green and Reed 1998), modulation of cellular defense mechanisms, and adaptive responses (Erusalimsky and Moncada 2007). Mitochondria appear to be one of the most sensitive targets for AgNP toxicity (Ahamed et al. 2010). Nanoparticle-induced impairment of the mitochondrial function has important biologic effects, which include the initiation of apoptosis and decreased adenosine triphosphate (ATP) production (Hiura et al. 2000).

Mitochondrial ATP synthase/ATPase (ATP hydrolase: EC 3.6.1.34) is an enzyme complex, responsible for ATP synthesis. It is comprised of a membrane-spanning sector F_0 and a soluble sector F_1. The latter catalyzes the synthesis of ATP from adenosine diphosphate (ADP) and inorganic phosphate (Pi) by utilizing the transmembrane proton gradient and membrane potential generated during substrate oxidation. This reaction can be reversed by pumping protons in the opposite direction resulting in ATP hydrolysis (Boyer 1997). A number of recent studies have focused on the cytotoxicity of nanoparticles with respect to changes in cell morphology, cell viability, metabolic activity, and oxidative stress (AshaRani et al. 2009; Carlson et al. 2008; Chairuangkitti et al. 2013; Hussain et al. 2005; Piao et al. 2011). Although limited studies have demonstrated that nanoparticles impair the mitochondrial oxidative phosphorylation capacity by inhibiting the respiratory chain and/or uncoupling between the oxidation and the phosphorylation (Costa et al. 2010; Teodoro et al. 2011), there are no reports on direct or indirect effects of AgNPs on the mitochondrial ATPase activity.

Several factors have been reported to influence AgNP toxicity such as particle size, shape, surface area, capping agents, and surface reactivity. In general, smaller nanoparticles were found to be more toxic, compared with larger nanoparticles (Kim et al. 2012; Panda et al. 2011). A smaller diameter of spherical particles is related with an increased surface-to-volume ratio and, in turn, the increased surface area is accompanied by increased chemical reactivity (Elsaesser and Howard 2012; Nel et al. 2009). The chemical nature of the capping agent on the nanoparticle surface was also found to be important, since the colloidal stability and the interactions of nanoparticles with cell membranes depend largely on the nanoparticles' surface properties (Elsaesser and Howard 2012). Moreover, some capping agents are more toxic than others (Lima et al. 2012). Hence, the design of synthesis methods using environmentally benign solvents and nontoxic chemicals for preparation of AgNPs has become a major field of interest. The green synthesis of AgNPs involves three main steps, which must be evaluated based on green-chemistry perspectives, including (i) selection of solvent medium, (ii) selection of environmentally benign reducing agent, and (iii) selection of nontoxic substances for the AgNPs stability (Raveendran et al. 2003). The green-chemistry type AgNPs synthesis processes have been reviewed by Sharma et al. (2009) and include mixed-valence polyoxometallates, polysaccharides, Tollens' reagents, irradiation, and biological methods. Silver nanocomposites containing carbohydrates and biopolymers have a relatively large potential due to their biocompatibility, low cost, and green approach (Dallas et al. 2011). Starch-coated AgNPs were found to be toxic for cells (Ahamed et al. 2008, 2010; AshaRani et al. 2008, 2009). While polysaccharide-coated nanoparticles are widely applied and investigated, data concerning nanoparticles stabilized with other saccharides are scarce.

In this regard, we synthesized, characterized, and evaluated the in vitro effects of AgNPs of two different sizes ($D_{av} = 15.4 \pm 3.9$ nm and $D_{av} = 24.8 \pm 6.8$ nm), electrosterically stabilized with various nontoxic environmental friendly capping agents (the polysaccharide starch and trisaccharide raffinose, respectively) with an emphasis

on their potential action on rat liver mitochondrial ATPase. This could contribute to the elucidation of the mechanisms underlying AgNPs toxicity.

Materials and methods

Chemicals

Sucrose, potassium chloride (KCl), magnesium chloride ($MgCl_2$), potassium dihydrogen phosphate (KH_2PO_4), sulfuric acid (H_2SO_4), sodium deoxycholate ($C_{24}H_{39}NaO_4$), iron(II) sulfate heptahydrate ($FeSO_4{\cdot}7H_2O$), ammonium molybdate ($H_2SO_4(NH_4)_6Mo_7O_{24}{\cdot}4H_2O$), and Folin reagent were purchased from Merck (Germany). Adenosine-5′-triphosphate disodium salt (ATP) and Tris(hydroxymethyl)aminomethane (Tris) were obtained from Sigma Aldrich (USA); potassium hydroxide (KOH), sodium hydroxide (NaOH), and L-cysteine—from Fluka (Switzerland); ethylenediaminetetraacetate disodium salt (EDTA), bovine serum albumin (BSA)—from Serva (USA); perchloric acid ($HClO_4$)—from Riedel de Haën (Germany); 2,4-dinitrophenol (DNP)—from BDH (England). Silver nitrate ($AgNO_3$, 99.8 %, Merck, Germany), soluble starch (Merck, Germany), pharmaceutical grade D-(+) glucose, D-(+) raffinose pentahydrate (Alfa Aesar, Germany), and sodium hydroxide (NaOH, 99 %, Merck, Germany) were used to prepare aqueous dispersions of AgNPs. All other chemicals were of reagent grade. Fresh stock solutions of ATP and cysteine were prepared prior to each experiment and kept on ice to preserve them from hydrolysis and oxidation, respectively. Double distilled water was used for preparation of all reagent solutions.

Animals

Liver mitochondria were isolated from male albino rats (Wistar strain; 50–60 days of age; 120–150 g; supplied by Experimental and Breeding Base for Laboratory Animals, Slivnitsa, Bulgaria). The animals received a standard laboratory diet (commercial rat chow, TopMix Ltd., Bulgaria) and water ad libitum and were fasted prior to use. They were decapitated and the liver was surgically removed for subsequent isolation of hepatic mitochondria. All studies were performed in accordance with the institutional ethical guidelines.

Synthesis of AgNPs

AgNPs were synthesized and characterized in the Laboratory of Nanoparticle Science and Technology, Department of General and Inorganic Chemistry, Faculty of Chemistry and Pharmacy, Sofia University "St. Kliment Ohridski". Starch-stabilized AgNPs (AgNPs/Starch) and raffinose-stabilized AgNPs (AgNPs/Raff) were prepared by one-step, one-phase "green" synthesis based on chemical reduction methods in aqueous solutions.

AgNPs/Starch were synthesized by reduction of Ag^+ ($AgNO_3$, 0.001 M) using D-(+) glucose (0.1 M) as a reducing agent, soluble starch (0.2 %, w/v) as a stabilizing agent, and sodium hydroxide (0.1 M) as a reaction catalyst (Vasileva et al. 2011). Briefly, 20 ml of $AgNO_3$ solution were added to 40 ml of starch solution, homogenized in an ultrasonic environment (power 100 W, frequency 38 MHz) for 15 min followed by the addition of 600 µl of D-(+) glucose solution and 3 ml of sodium hydroxide solution. The reaction mixture was incubated in an ultrasonic environment at 30 °C for 60 min. The color of the solution changed immediately from colorless to pale brown and subsequently to light yellow, indicating nanoparticle formation.

AgNPs/Raff were obtained by reduction of Ag^+ ($AgNO_3$, 0.1 M) using D-(+) raffinose (0.1 M) both as reducing and stabilizing agent, and sodium hydroxide (0.1 M) as a reaction catalyst. Briefly, 5 ml of raffinose solution and 0.5 ml of $AgNO_3$ solution were added to 40.5 ml of distilled water, homogenized in an ultrasonic environment for 15 min followed by the addition of 4 ml of sodium hydroxide solution. The reaction mixture was kept in an ultrasonic environment at 30 °C for 60 min. A change of the solution color from colorless to pale brown and subsequently to yellow orange was observed, indicating nanoparticle formation.

Using the methods described above, starch- and raffinose-stabilized AgNPs were obtained with Ag concentrations of 3×10^{-4} mol/l (32 mg/l) and 1×10^{-3} mol/l (110 mg/l), respectively. AgNPs/Starch and AgNPs/Raff primary dispersions were centrifuged at 14,000 rpm for 90 and 60 min, respectively. The supernatants containing soluble

components of the reaction mixtures were decanted and the nanoparticle pellets were re-dispersed using sonication in tenfold and sixfold less volume of double distilled water for AgNPs/Starch and AgNPs/Raff, respectively. As a result of the described procedures, concentrated stock dispersions of starch- and raffinose-stabilized AgNPs were obtained with silver concentrations of 3×10^{-3} mol/l (320 mg/l) and 6×10^{-3} mol/l (650 mg/l), respectively. This step ensured purification of the nanoparticles employed in the study by elimination of the reaction side products. The stock dispersions were kept in closed containers at room temperature and used after appropriate dilutions in the following experiments. The nanoparticle dispersions were homogenized by an ultrasonic bath UST2.4-150 (Siel, Bulgaria) for 30 min prior to each experiment.

Characterization of AgNPs

The aqueous dispersions of AgNPs were characterized by UV–Visible spectroscopy using an Evolution 300 spectrometer (Thermo Scientific, USA). Double distilled water was used as a reference for the base line. The formation of AgNPs was further confirmed by X-ray diffraction (XRD). Briefly, 2 ml of AgNP suspension (on portions of 100 µl) were placed on microscope glass and air-dried. The XRD patterns of the dried samples were determined using an X-ray powder diffractometer (Siemens D500) equipped with CuKα radiation ($\lambda = 1.54$ Å) in 2θ ranging from 15° to 80°. In addition, the morphology and particle sizes were examined using a transmission electron microscope (TEM, JEM-2100) operating at accelerating voltage of 200 kV. Volume of 5 µl AgNP suspension was placed on a carbon-covered copper grid for TEM and then air-dried. Size distribution of the nanoparticles and average particle size were determined from the TEM images for at least 200 particles using imaging software (Image J). Zeta (ζ) potential of AgNPs was measured with a Zetasizer Nano ZS (Malvern) instrument.

Isolation of rat liver mitochondria

Intact mitochondria were isolated by the method of Johnson and Lardy (1967) with modifications. Briefly, livers were repeatedly washed in icy isolation medium consisting of 0.25 M sucrose and 1 mM EDTA-KOH (pH 7.5) and homogenate (in proportion tissue to medium 1:3) was prepared using a Potter–Elvehjem type glass-Teflon homogenizer. The homogenate was centrifuged at $600\times g$ for 10 min and the resulting supernatant was retained. The pellet was further re-suspended and centrifuged under the same conditions. The combined supernatants were centrifuged at $14{,}000\times g$ for 10 min. The resulting pellet was suspended in washing medium consisting of 0.25 M sucrose (to 1/3 of the initial volume) and further centrifuged under the same conditions. The final mitochondrial pellet was suspended in 1–1.5 ml washing medium. All operations were carried out at 0–4 °C. The mitochondria thus obtained were used within 4 h or kept at −15 to 20 °C. Following freezing/thawing the mitochondria uncouple and can be used for ATPase activity assay or for the isolation of submitochondrial particles (SMPs). Mitochondrial protein was determined by the biuret reaction with BSA as a reference standard.

Isolation of submitochondrial particles

SMPs were isolated by the method of Racker and Horstmann (1967) with modifications. The mitochondrial suspension was diluted with medium consisting of 0.25 M sucrose and 5 mM EDTA-KOH (pH 7.5) to a protein concentration of 8-10 mg/ml. The suspension was adjusted to pH 9.2 with 1 M NH_4OH. Subfractionation of mitochondria was performed by six periods of sonification for 30 s with 1 min intervals between them, using an ultrasonic disintegrator Soniprep-150 (MSE Ltd., UK). During sonification the suspension temperature was kept at 0–4 °C. After that the suspension was centrifuged at $26{,}000\times g$ for 15 min, the resulting supernatant was adjusted to pH 6.2 and further centrifuged at $25{,}000\times g$ for 45 min. The pellet of SMPs was suspended in 0.25 M sucrose to the initial volume and centrifuged under the same conditions. The final pellet of ammonium SMPs was suspended in 0.25 M sucrose to a protein concentration of 10–20 mg/ml and was kept at −20 °C. Protein concentration was determined by the method of Lowry et al. (1951) with BSA as a reference standard.

Assay of ATPase activity

ATPase activity was determined by measurement of Pi released from ATP. The reaction with the freeze-

thawed mitochondria was carried out in 1 ml reaction medium consisting of 0.2 M sucrose, 10 mM KCl, 50 mM Tris–HCl, and 100 μM EDTA-KOH, pH 7.5. Aliquots of the AgNPs stock solution were added to reach final concentrations of 3, 10, 25, and 50 mg/l respectively. After pre-incubating the mitochondria in the assay medium for 10 min at 37 °C the reaction was initiated by the addition of 1 mM ATP (final concentration), continued for 5 min and terminated by adding 0.4 ml of 3 M perchloric acid.

The assay medium for SMPs had the same composition except that 2 mM $MgCl_2$ was added since these preparations lose bound Mg^{2+} during isolation. Other experimental conditions were as previously described.

The ATPase reaction with intact mitochondria was carried out at room temperature and continuous stirring in 5 ml assay medium consisting of 0.2 M sucrose, 10 mM KCl, 50 mM Tris–HCl, 100 μM EDTA-KOH, and 1 mM ATP (pH 7.5) and 50 μM DNP was included wherever indicated. Aliquots of the AgNPs stock solution were added to reach final concentrations of 25 and 50 mg/l respectively. The reaction was started by adding the mitochondrial suspension. Samples of 500 μl were taken after 30, 60, 120, 180, 300, and 600 s incubation and added to 200 μl of 3 M perchloric acid for termination of the reaction.

In all cases the protein precipitates and nanoparticles were removed by centrifugation at 8,800×g for 30 min. The concentration of Pi in the supernatant was determined spectrophotometrically (spectrophotometer S-22UV/Vis, Boeco, Germany) at $\lambda = 750$ nm using the method of Fiske and Subbarow (1925) with modifications. Blanks in which the reaction was blocked by addition of perchloric acid before ATP addition were carried out in parallel in order to determine the background Pi amount as a result of non-enzymatic hydrolysis. The activity of mitochondrial ATPase was expressed as μmol Pi mg/protein min or μmol Pi mg/protein.

Statistical analysis

Data are expressed as mean ± standard error of the mean (SEM) of at least three independent experiments performed in duplicate unless otherwise indicated.

When appropriate, the difference between nanoparticles-treated samples and the untreated control was tested by one-way analysis of variance (ANOVA) followed by Tukey test with treatment as a factor. For one of the groups Kolmogorov–Smirnov test showed that the data were not normally distributed and non-parametric Kruskal–Wallis one-way ANOVA on Ranks test was performed. A value of $p < 0.05$ was considered significant. All statistical analyses were computed using SigmaStat version 3.5.

Results and discussion

Two types of nanoparticles, starch- and raffinose-stabilized AgNPs, were successfully synthesized by green-chemical reduction methods, using glucose and raffinose, respectively, as reducing agents in alkaline aqueous solutions. The effects of the two types of AgNPs on the ATPase activities of three different mitochondrial preparations were investigated: (i) intact mitochondria (coupled mitochondria); (ii) freeze-thawing disrupted mitochondria; and (iii) SMPs.

Our previous experiments (unpublished data) demonstrated that oligomycin, a specific inhibitor of F-ATPases, in concentration of 1 μg/mg protein significantly inhibited the ATPase activity of freeze-thawed mitochondria in control conditions ($p = 0.014$, $n = 3$). Oligomycin-sensitive ATPase activity was calculated as the difference in the activity in the absence (total ATPase activity) and presence of oligomycin (oligomycin-insensitive). The results showed that 84.94 ± 2.04 % of the total mitochondrial ATPase activity were oligomycin-sensitive. This allowed us to accept that the largest part of the registered mitochondrial ATPase activity was oligomycin-sensitive and the contribution of other ATPases was negligible.

There are no data that the stabilizing agents, raffinose and starch, can influence the mitochondrial ATPase activity. It has been demonstrated that sucrose, dextrose, fructose, lactose, arabinose, and raffinose had either no effect on mitochondrial ATPase from rat liver or else caused only a small inhibition (Ulrich 1964). Furthermore, when starch alone was used as control, no significant cytotoxicity was found in both cancer cells and fibroblasts, which illustrates the biocompatibility of starch as a capping agent in nanoparticles (AshaRani et al. 2009).

Nanoparticle characterization

Optical characteristics and stability of the nanoparticle dispersions at storage and after concentration

UV–Vis absorption measurements of the primary yellow solutions of starch- and raffinose-stabilized AgNPs showed UV–Visible spectra with surface plasmon resonance (SPR) bands at λ_{max} of 410 and 413 nm, respectively (Figs. S1a and S1b). The registered reproduction of the optical characteristics (SPR maximum and full band width at half maximum, FWHM) of the nanoparticles in the concentrated aqueous dispersions demonstrated their high colloidal stability after the concentration by centrifugation (Fig. S1c). Practically, the absorption spectra of the two types of nanoparticles coincided, i.e., broader FWHM of AgNPs/Starch was observed after the concentration procedure in comparison with UV–Vis spectrum of primary solutions of starch-stabilized AgNPs shown in Fig. S1a. This could be explained by the fact that during centrifugation of the starch-stabilized nanoparticles, even with a duration of 90 min, the smallest particles did not precipitate and remained in the supernatant (supernatants were pale yellow solutions). Hence, this fraction of smallest nanoparticles was not present in the concentrated aqueous dispersion of AgNPs/Starch.

Morphology and crystal structure

It can be seen from TEM micrographs (Fig. 1) and UV–Vis spectra (Fig. S1) that aqueous dispersions of starch- and raffinose-stabilized AgNPs with a relatively narrow size distribution and high colloidal stability at storage can be obtained. The colloidal stability of the two types of AgNPs synthesized was also confirmed by the ζ potential values of -25.3 ± 1.3 mV (AgNPs/Starch) and -47.2 ± 1.1 mV (AgNPs/Raff) measured in 1 mM KCl at pH 6.8. TEM measurements showed that the resulting products mainly consisted of quasi-spherical nanoparticles with average size of 15.4 ± 3.9 nm for AgNPs/Starch, and of 24.8 ± 6.8 nm for AgNPs/Raff. In addition to the nanospheres, some typical polyhedral nanoparticles (multiple twined nanocrystals) can be easily observed.

The XRD pattern of AgNPs/Starch (Fig. 2a) revealed three broad diffraction peaks with very weak

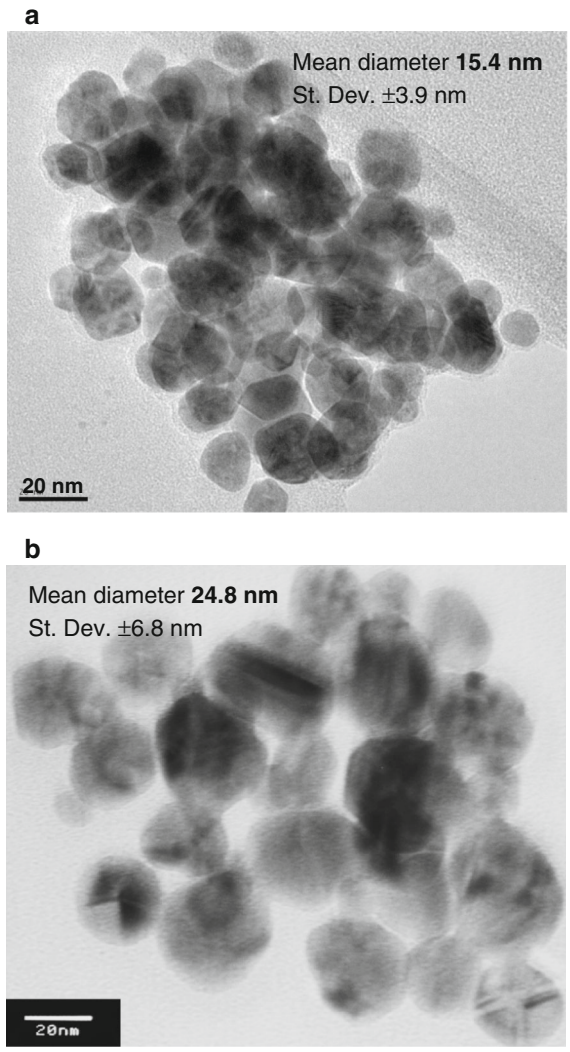

Fig. 1 Transmission electron microscope (TEM) images of starch-stabilized (AgNPs/Starch, **a**) and raffinose-stabilized silver nanoparticles (AgNPs/Raff, **b**). TEM measurements showed that the resulting products mainly consisted of quasi-spherical nanoparticles with average size of 15.4 ± 3.9 nm for AgNPs/Starch, and of 24.8 ± 6.8 nm for AgNPs/Raff

intensity indicating the amorphous nature of AgNPs–starch complexes, comprising polycrystalline nanoparticles with fine nanocrystallite nature. The XRD pattern of AgNPs/Raff (Fig. 2b) showed four relatively broad diffraction peaks with 2θ of 38.2°, 44.4°, 64.6°, and 77.4° corresponding to the (111), (200), (220), and (311) planes respectively, of the face-centered cubic (fcc) silver, confirmed by SAED pattern from TEM observations (not shown). No impurity peaks were observed in the XRD patterns of both types of nanoparticles.

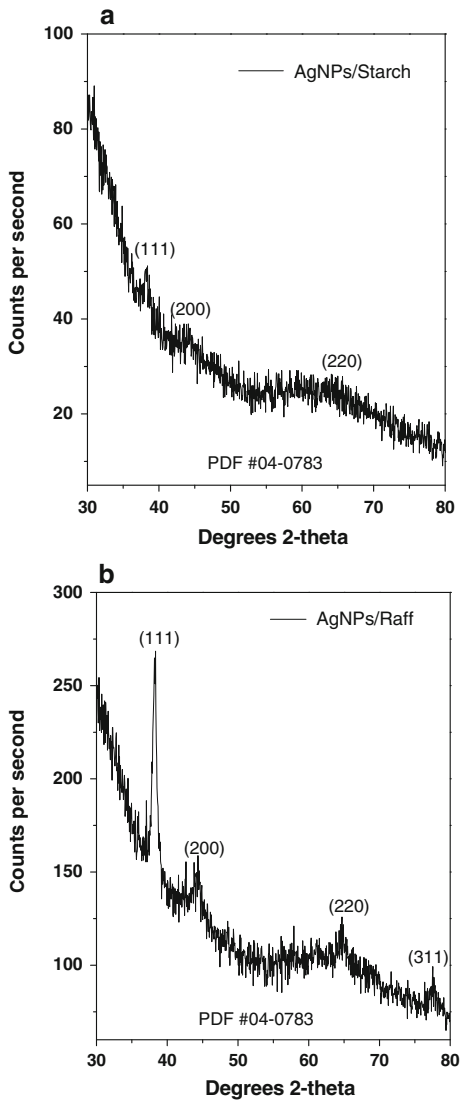

Fig. 2 X-ray diffraction patterns of starch-stabilized (**a**) and raffinose-stabilized (**b**) silver nanoparticles. The abbreviations are the same as in Fig. 1

Effects of raffinose- and starch-stabilized silver nanoparticles on intact mitochondria

To test the possible uncoupling action of the nanoparticles a set of experiments with intact mitochondria was carried out. Figure 3a and b show the results from one representative experiment with raffinose-stabilized AgNPs applied in concentrations of 25 mg/l and 50 mg/l. ATPase activity remained low during the registration for 600 s under control conditions. Addition of the uncoupler DNP in final concentration of 50 μM powerfully stimulated ATP hydrolysis. The effects of AgNPs/Raff were similar, indicating their uncoupling action on intact mitochondria (Fig. 3a). We could not obtain convincing data about the influence of AgNPs/Raff on ATPase activity of DNP-uncoupled mitochondria (Fig. 3b).

The effects of AgNPs/Starch on ATPase activity of intact mitochondria are presented in Fig. 3c and d. Addition of the nanoparticles in concentrations of 25 and 50 mg/l led to strong stimulation of ATP hydrolysis similarly to the effect of DNP in concentration of 50 μM (Fig. 3c). These results confirmed the uncoupling action of the AgNPs on mitochondria. Unlike AgNPs/Raff effects, AgNPs/Starch reduced DNP-stimulated ATPase activity (Fig. 3d). This suggests that starch-stabilized AgNPs are able to pass the mitochondrial membrane with subsequent inhibition of ATPase activity.

Data have been presented that AgNPs do penetrate the cell membranes although the exact mechanisms have not been clearly identified (Diaz et al. 2008; Piao et al. 2011). Hussain et al. (2005) showed that at a low dose (10 μg/ml) AgNPs associated with the cell membranes and with increasing doses the cells internalized particles and became irregular in shape. The mechanism of AgNP cellular entry could involve large-scale phagocytosis of agglomerates or a passive, nonspecific diffusion of individual particles through the cell membrane (Carlson et al. 2008).

Effects of raffinose- and starch-stabilized AgNPs on freeze-thawed mitochondria and SMPs

Freezing/thawing disrupts the mitochondrial inner membrane leading to uncoupling and stimulation of initial ATPase activity. In parallel with this, mitochondria preserve their structure and the membrane-spanning F_0 sector of the ATPase.

ATPase activity values were calculated as percentages of the activity (expressed as μmol Pi mg/protein·min) measured under control conditions (nanoparticle-free assay medium). AgNPs/Raff in concentrations of 3, 10, 25, 50 mg/l reduced ATPase activity of freeze-thawed mitochondria in a dose-dependent manner (to 78.60 ± 8.64 % of the control), but the differences between the groups were not statistically significant (Fig. 4a). In contrast, AgNPs/Starch significantly inhibited ATPase

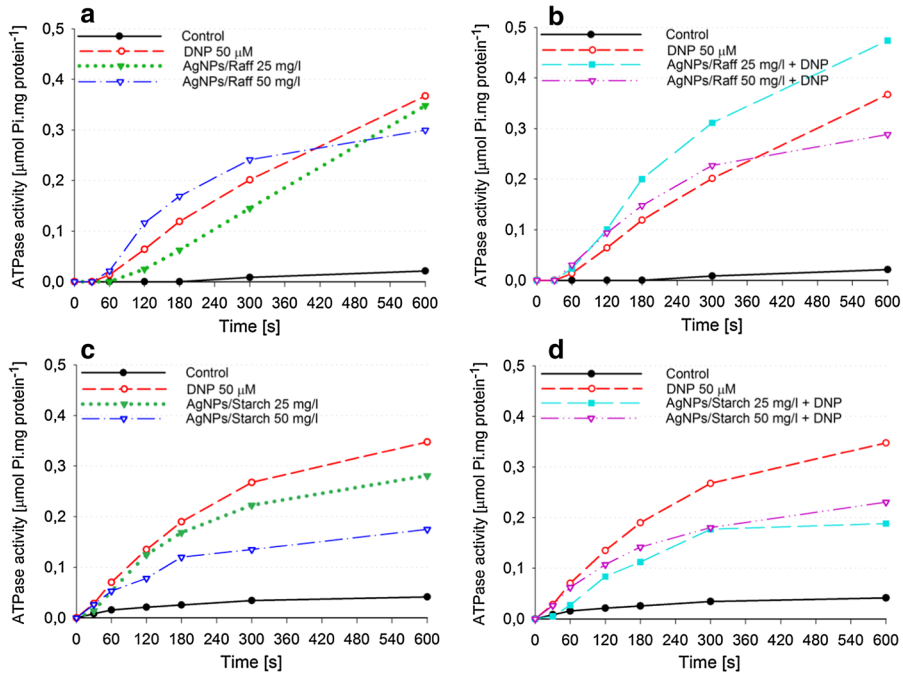

Fig. 3 Effects of AgNPs/Raff on ATPase activity of intact (**a**) and 2,4-dinitrophenol (DNP)-uncoupled mitochondria (**b**); **c** effects of AgNPs/Starch on ATPase activity of intact mitochondria; **d** effect of AgNPs/Starch on DNP-uncoupled mitochondria. The reactions were started by adding 80 μl of mitochondrial suspension (protein 5.2 mg/sample and 9.4 mg/sample for AgNPs/Raff and AgNPs/Starch, respectively) and carried out for 10 min as described in "Materials and methods" section. Data present curves registered during one experiment with AgNPs/Raff and AgNPs/Starch, respectively. The abbreviations are the same as in Fig. 1

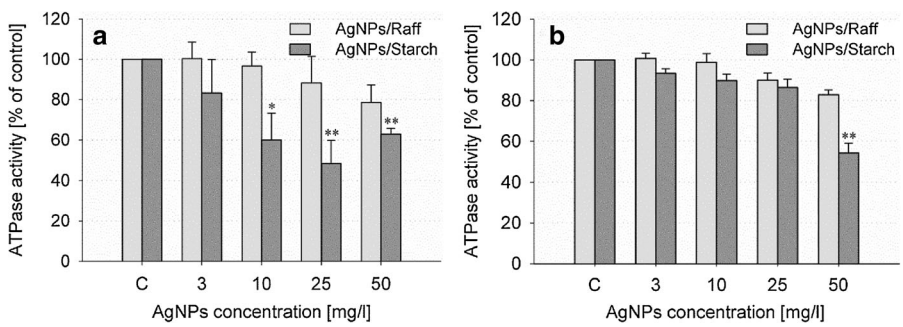

Fig. 4 Effect of AgNPs/Raff and AgNPs/Starch on ATPase activity of freeze-thawed mitochondria (**a**) and submitochondrial particles (SMP, **b**). ATPase activity values were calculated as percentages of the activity measured under control conditions (nanoparticle-free assay media, *C*). Data in **a** are plotted as mean ± SEM of six (for AgNPs/Raff) and five (for AgNPs/Starch) independent experiments (two parallel samples per group per experiment). Data in **b** are plotted as mean ± SEM of seven (for AgNPs/Raff) and nine (for AgNPs/Starch) independent experiments (two parallel samples per group per experiment). The difference between nanoparticles-treated samples and the untreated control was tested by one-way analysis of variance (ANOVA) followed by a Tukey test with "treatment" as the independent factor. For the group of mitochondria treated with AgNPs/Starch, 25 mg/l, the Kolmogorov–Smirnov test showed that the data were not normally distributed; hence, a non-parametric Kruskal–Wallis one-way ANOVA test on ranks was performed. *Asterisks* indicate significant differences (*$p < 0.05$; **$p < 0.01$) from the control. The abbreviations are the same as in Fig. 1

activity, as the strongest effect was observed at concentration of 25 mg/l – 48.28 ± 11.43 % of the control.

These results supplement the data on possible deleterious effects of AgNPs in cells. A study on normal human lung fibroblast cells and human

glioblastoma cells has shown the toxicity of starch-coated AgNPs in which the proposed possible mechanism involves disruption of the mitochondrial respiratory chain by AgNPs leading to production of reactive oxygen species, interruption of ATP synthesis and DNA damage (AshaRani et al. 2009). Impaired oxidative phosphorylation capacity has also been demonstrated in rat liver mitochondria exposed to AgNPs mainly due to alterations of mitochondrial membrane permeability (Teodoro et al. 2011). However, the authors have not found any changes in the activity of several enzymatic chain complexes and in the ATP levels. On the other hand, in vitro experiments have demonstrated inhibition of the activities of respiratory chain complexes I, II, III, and IV from rat liver, induced by AgNPs in concentrations similar to those used in our experiments (Costa et al. 2010). AgNPs-caused impairment of the mitochondrial function could involve damage of the inner mitochondrial membrane. It is suggested that AgNPs may affect cellular enzymes by interference with free thiol groups and via mimicry of endogenous ions (Chen and Schluesener 2008; Völker et al. 2013).

The observed effects of the AgNPs could be due to direct interactions with the water-soluble catalytic complex F_1 and/or with the membrane sector F_0. For partial localization of the site of action of the nanoparticles series of experiments with SMPs were carried out. SMPs represent closed inverted vesicles derived from the inner mitochondrial membrane. As a result, the complex F_1 is located on the outside of the membrane and oriented to the solution, which allows direct access of the reagents in the medium to the enzyme. Due to absence of a membrane, some of the properties of ATPase from SMPs resemble those of the soluble mitochondrial ATPase (F_1). In our opinion, SMPs are a suitable instrument for investigating the activity of the membrane-bound mitochondrial ATPase without the limitation of the outer mitochondrial membrane. The results obtained with SMP (Fig. 4b) were similar to those from the experiments with freeze-thawed mitochondria. The ATPase activity of SMPs was slightly decreased by AgNPs/Raff (to 82.76 ± 2.46 % of the control), whereas AgNPs/Starch in concentration of 50 mg/l significantly inhibited the activity to 54.22 ± 4.86 % ($p = 0.006$).

Overall, our finding that both types of AgNPs increased the rate of ATP hydrolysis in intact mitochondria showed that they were able to change the permeability of the mitochondrial membrane. The observed identical inhibitory effects of AgNPs/Starch on the ATPase activity of DNP-stimulated mitochondria (uncoupled mitochondria), freeze-thawed (disrupted) mitochondria, and SMPs indicated that the mitochondrial membrane was not a barrier for the nanoparticles to enter the mitochondria and interact directly with the enzyme. Since in the lower concentrations (10 and 25 mg/l) of starch-stabilized AgNPs a weaker effect on the SMP activity was observed compared to that in freeze-thawed mitochondria, it could be assumed that the outer mitochondrial membrane was a nanoparticle target structure as well.

The established different effects of the two types of AgNPs could be due to the difference in their size and/or the stabilizing agents used for synthesis (Ahamed et al. 2008, 2010; Samberg et al. 2010). Starch as a polysaccharide with helical structure forms a thicker coating on AgNPs surface than the trisaccharide raffinose does. On the other hand, the starch-stabilized AgNPs are smaller than AgNPs/Raff (15.4 ± 3.9 and 24.8 ± 6.8 nm, respectively). Thus, the more significant effects of AgNPs/Starch compared to AgNPs/Raff could be assigned mainly to their smaller size. Hence, the nanoparticle size appears to be the dominant factor determining the nanoparticle reactivity and the observed effects on the mitochondrial ATPase activity. This conclusion is in accordance with recently reported data. It has been found that smaller AgNPs are able to penetrate the mammalian cell membrane more efficiently than larger AgNPs. These AgNPs also cause more significant cytotoxicity than larger AgNPs because of their larger surface area available for interaction with cellular organelles (Kim and Ryu 2013; Liu et al., 2010).

Influence of cysteine on the effects of AgNPs on ATPase activity of submitochondrial particles

In aqueous solutions Ag^+ could be released by surface oxidation of AgNPs (Kim et al. 2009; Kim and Ryu 2013) and the mechanisms of AgNPs cytotoxicity can also be referred to Ag^+ (Chen and Schluesener 2008). There are data suggesting that the Ag^+ ion is the actual species that accounts for the toxicity of AgNPs (Limbach et al. 2007; Lubick 2008; Park et al. 2010; Yang et al. 2012). Other studies indicate that AgNPs toxicity is associated with production of Ag^+ but these ions could not fully explain AgNPs biological effects

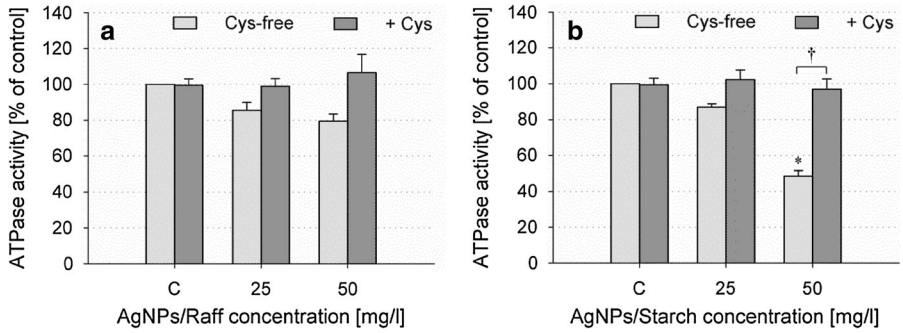

Fig. 5 Influence of cysteine (*Cys*) on the effects of AgNPs/Raff (**a**) and AgNPs/Starch (**b**) on the ATPase activity of submitochondrial particles. ATPase activity values were calculated as percentages of the activity measured under control conditions (nanoparticle-free assay media, *C*). Data are plotted as mean ± SEM of three independent experiments (two parallel samples per group per experiment). The differences between the groups were tested by ANOVA followed by a post hoc Tukey test. $*p < 0.05$—significant differences from the control; † $p < 0.05$—significant differences from the cysteine-free media. The abbreviations are the same as in Fig. 1

(Kawata et al. 2009; Kim et al. 2009). In fact, AgNPs and Ag^+ exert similar biological effects (Foldbjerg et al. 2009; Laban et al. 2010; Miura and Shinohara 2009). For example, Ag^+ exhibits a high affinity to thiol groups of cysteine residues in membrane-bound enzymes and proteins (Holt and Bard 2005; Liau et al. 1997; Zeiri et al. 2004) similar to AgNPs effects on cellular enzymes (Chen and Schluesener 2008; Völker et al. 2013). Therefore, it is necessary to distinguish the toxic effects of AgNPs and Ag^+ (Johnston et al. 2010). An useful tool to examine the contribution of Ag^+ to the overall toxicity of AgNPs is cysteine, a strong Ag^+ ligand (Navarro et al. 2008). In this study, 5 mM L-cysteine was used as an Ag^+ ligand to assess the contribution of these ions to AgNPs effects on the mitochondrial ATPase activity. As can be seen in Fig. 5, cysteine alone did not affect the ATPase activity of SMPs, but it completely abolished the inhibitory effect of starch-stabilized AgNPs. With respect to AgNPs/Raff, the data obtained in the whole concentration range studied did not show statistically significant differences from the control.

Similar effects of cysteine on the toxicity of AgNPs have been previously reported. Navarro et al. (2008) found that cysteine abolished the inhibitory effects of AgNPs on photosynthesis in algae, *Chlamydomonas reinhardtii* and concluded that AgNPs contributed to the toxicity as a source of ionic Ag^+. Kawata et al. also suggested that Ag^+ contributes mainly to the cytotoxic and stress-associated effects of AgNPs.

Taking into account the studies and discussions of other researchers (AshaRani et al. 2008; Lim et al. 2012, Nair et al. 2010) regarding the contribution of Ag ions obtained by AgNP dissolution to nanoparticle toxicity, we can assume that the concentration of released Ag^+ in our experimental conditions was low enough to exclude the possibility that this was a major factor in AgNPs effects. Thus, the question arises as to whether the abolishment of AgNPs effects by cysteine is a result of its interaction with the nanoparticles themselves causing their aggregation. Therefore, the nanoparticle stability in the medium used is an important factor that can influence AgNPs effects on the ATPase activity.

Stability of AgNP in the reaction medium

Since nanoparticles are liable to display different aggregation states depending on their chemical environment, their characterization in the medium used for the experiments is particularly important (Navarro et al. 2008). In this connection, UV–Visible absorption spectra of AgNPs were measured in the reaction media used in the present experiments. UV–Visible absorption spectra and photographs of AgNPs/Starch added to reaction media with different composition are presented in Fig. 6a. We found that starch-stabilized AgNPs were characterized by colloidal stability in both reaction media with and without the substrate ATP. In a reaction medium containing cysteine, lowering of the SRP absorption intensity at 400 nm (transverse SRP) and a new band at about 530 nm (longitudinal SRP) can be observed. This corresponds to a change of the solution color from yellow to pink-red.

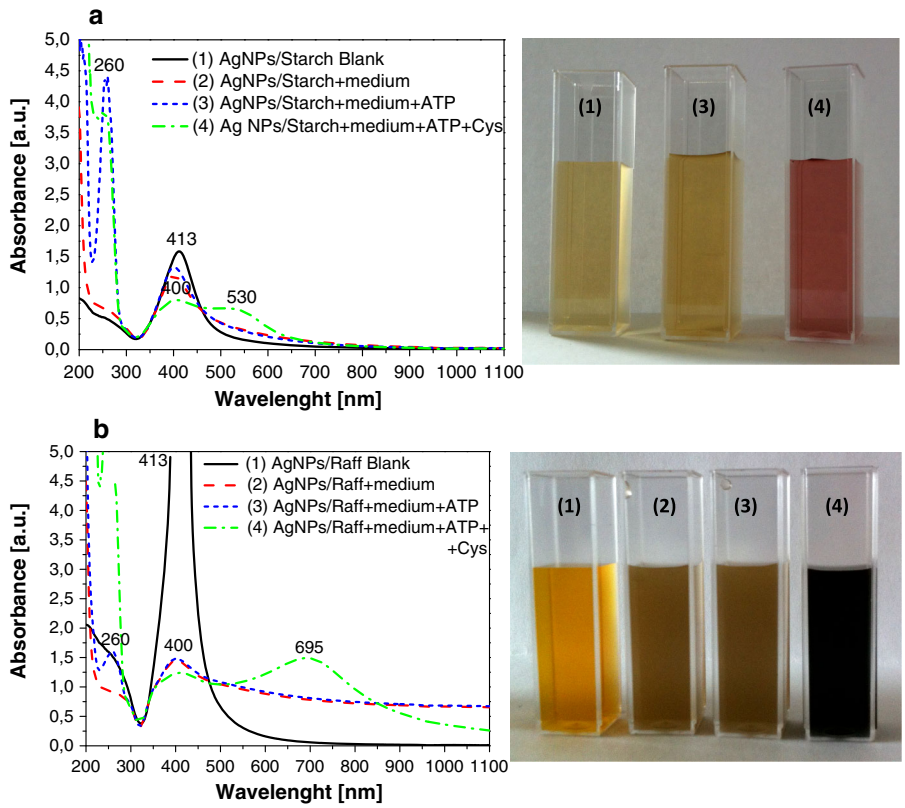

Fig. 6 UV–Visible absorption spectra and photographs recorded after adding of AgNPs/Starch (**a**) and AgNPs/Raff (**b**) to double distilled water (*1*); a reaction medium (*2*); a reaction medium, containing adenosine triphosphate (ATP, *3*); and a reaction medium, containing ATP and cysteine (*4*). The abbreviations are the same as in Fig. 5

UV–Vis absorption spectra and the photograph presented in Fig. 6b show that AgNPs/Raff possess lower colloidal stability in the reaction medium used, as well as in the reaction medium containing ATP. This is the reason for the enhanced background absorption at wave lengths above 450 nm and the evident change of the solution color from yellow to light brown. These results suggest nanoparticle aggregation and thus a reduction in reactivity. Notably, in a reaction medium containing cysteine SRP absorption intensity at 400 nm (transverse SRP) was decreased and a second band at 695 nm (longitudinal SRP) appeared which correspond to a change of the solution color to deep blue.

The changes in AgNPs optical characteristics in a medium containing cysteine may be due to chemisorption of cysteine on the surface of the nanoparticles and to formation of aggregates with an anisotropic shape. Formation of these large complexes could explain the cysteine-provoked abolishment of AgNPs inhibitory effects on ATPase activity. Compared to AgNPs/Starch, AgNPs/Raff aggregated to structures with larger size and greater degree of anisotropy as evident from the red-shift of the longitudinal SRP band in their spectrum. One possible explanation for this difference is that the particle surface of AgNPs/Raff was more accessible for cysteine molecules than that of AgNPs/Starch, resulting in accelerated aggregation for raffinose-stabilized AgNPs. Gondikas et al. (2012) have also discussed that along with the complexation of dissolved Ag^+, cysteine can induce aggregation of the nanomaterials, leading to a secondary mechanism by which the presence of cysteine could decrease the Ag NP toxicity. In addition, Xiu et al. (2011) have argued that using cysteine to neutralize Ag^+ may confound the reactivity of the AgNPs themselves due to their potential association with the added ligand. It has also been demonstrated that cysteine decreases the inhibitory effects of both Ag^+ and AgNPs (He et al. 2012).

It should be noted that in the present study we demonstrate the inhibitory effects of AgNPs on the ATPase activity of freeze-thawed mitochondria and SMPs, i.e., a membrane-bound enzyme. There is a possibility that AgNPs affect the enzyme surroundings rather than enzyme itself. Further studies on AgNPs influence on the activity of isolated soluble ATPase (F_1) could provide opportunity to localize more precisely the site of AgNPs action.

Conclusions

Our findings demonstrate that AgNPs studied inhibit the activity of rat liver mitochondrial ATPase. Both types of AgNPs (starch- and raffinose-coated) increase the rate of ATP hydrolysis in intact mitochondria as expected for an uncoupling agent. The observed identical inhibitory effects on the ATPase activity of DNP-stimulated mitochondria (uncoupled mitochondria), freeze-thawed (disrupted) mitochondria, and SMPs are indications that the mitochondrial membrane is not a barrier for the nanoparticles to enter the mitochondria and interact directly with the enzyme. These results provide an insight into the mechanisms of the possible deleterious effects of AgNPs on the cells, in particular on mitochondria. Starch-stabilized AgNPs exert more potent inhibition of the mitochondrial ATPase activity than AgNPs stabilized with raffinose. We suggest that this differential is due to the different sizes of the two types of AgNPs and/or to the stabilizing agents used for their synthesis, which determine AgNPs colloidal stability in the assay media. Starch as a polysaccharide covers more tightly the metal core of AgNPs than does the raffinose. As a result, raffinose-coated AgNPs are less potent in inhibiting the mitochondrial ATPase activity because of their higher ability to aggregate in the medium used. This study proves the necessity of further research on the importance of surface coatings of AgNPs and their interaction with cellular components.

References

Ahamed M, Karns M, Goodson M et al (2008) DNA damage response to different surface chemistry of silver nanoparticles in mammalian cells. Toxicol Appl Pharmacol 233:404–410

Ahamed M, AlSalhi S, Siddiqui MKJ (2010) Silver nanoparticle applications and human health. Clin Chim Acta 411:1841–1848

AshaRani PV, Wu YL, Gong Z, Valiyaveettil S (2008) Toxicity of silver nanoparticles in zebrafish models. Nanotechnology 19:255102

AshaRani PV, Mun GLK, Hande MP, Valiyaveettil S (2009) Cytotoxicity and genotoxicity of silver nanoparticles in human cells. ACS Nano 3:279–290

Boyer PD (1997) The ATP synthase—a splendid molecular machine. Ann Rev Biochem 66:717–749

Carlson C, Hussain SM, Schrand AM, Braydich-Stolle LK, Hess KL, Jones RL, Schlager JJ (2008) Unique cellular interaction of silver nanoparticles: size-dependent generation of reactive oxygen species. J Phys Chem B 112:13608–13619

Chairuangkitti P, Lawanprasert S, Roytrakul S, Aueviriyavit S, Phummiratch D, Kulthong K, Chanvorachote P, Maniratanachote R (2013) Silver nanoparticles induce toxicity in A549 cells via ROS-dependent and ROS-independent pathways. Toxicol In Vitro 27:330–338

Chen X, Schluesener HJ (2008) Nanosilver: a nanoproduct in medical application. Toxicol Lett 176:1–12

Costa CS, Ronconi VJV, Daufenbach JF, Gonçalves CL, Rezin GT, Streck EL, da Silva Paula MM (2010) In vitro effects of silver nanoparticles on the mitochondrial respiratory chain. Mol Cell Biochem 342:51–56

Dallas P, Sharma VK, Zboril R (2011) Silver polymeric nanocomposites as advanced antimicrobial agents: classification, synthetic paths, applications, and perspectives. Adv Colloid Interface Sci 166:119–135

Diaz B, Sánchez-Espinel C, Arruebo M, Faro J, de Miguel E, Magadán S, Yagüe C, Fernández-Pacheco R, Ibarra MR, Santamaría J, González-Fernández A (2008) Assessing methods for blood cell cytotoxic responses to inorganic nanoparticles and nanoparticle aggregates. Small 4: 2025–2034

Elsaesser A, Howard CV (2012) Toxicology of nanoparticles. Adv Drug Deliv Rev 64(2):129–137

Eom H-J, Choi J (2010) p38 MAPK activation, DNA damage, cell cycle arrest and apoptosis as mechanisms of toxicity of silver nanoparticles in Jurkat T cells. Environ Sci Technol 44:8337–8342

Erusalimsky JD, Moncada S (2007) Nitric oxide and mitochondrial signaling. From physiology to pathophysiology. Aterioscler Thromb Vasc Biol 27:2524–2531

Fiske CH, Subbarow Y (1925) The colorimetric determination of phosphorus. J Biol Chem 66:375–400

Foldbjerg R, Olesen P, Hougaard M, Dang DA, Hoffmann HJ, Autrup H (2009) PVP-coated silver nanoparticles and silver ions induce reactive oxygen species, apoptosis and necrosis in THP-1 monocytes. Toxicol Lett 190:156–162

Gondikas AP, Morris A, Reinsch BC, Marinakos SM, Lowry GV, Hsu-Kim H (2012) Cysteine-induced modifications of zero-valent silver nanomaterials: implications for particle surface chemistry, aggregation, dissolution, and silver speciation. Environ Sci Technol 46:7037–7045

Green DR, Reed JC (1998) Mitochondria and apoptosis. Science 281:1309–1312

He D, Dorantes-Aranda JJ, Waite TD (2012) Silver nanoparticle–algae interactions: oxidative dissolution, reactive oxygen species generation and synergistic toxic effects. Environ Sci Technol 46:8731–8738

Hiura TS, Li N, Kaplan R, Horwitz M, Seagrave J, Nel AE (2000) The role of a mitochondrial pathway in the

induction of apoptosis by chemicals extracted from diesel exhaust particles. J Immunol 165:2703–2711

Holt KB, Bard AJ (2005) Interaction of silver(I) ions with the respiratory chain of *Escherichia coli*: an electrochemical and scanning electrochemical microscopy study of the antimicrobial mechanism of micromolar Ag^{+}. Biochemistry 44:13214–13223

Hussain SM, Hess KL, Gearhart JM, Geiss KT, Schlager JJ (2005) In vitro toxicity of nanoparticles in BRL 3A rat liver cells. Toxicol In Vitro 19:975–983

Johnson D, Lardy HA (1967) Isolation of liver or kidney mitochondria. In: Estabrook RW, Pullman ME (eds) Methods of enzymology, vol 10. Academic Press, New York, pp 94–95

Johnston HJ, Hutchison G, Christensen FM, Peters S, Hankin S, Stone V (2010) A review of the in vivo and in vitro toxicity of silver and gold particulates: particle attributes and biological mechanisms responsible for the observed toxicity. Crit Rev Toxicol 40:328–346

Kawata K, Osawa M, Okabe S (2009) In vitro toxicity of silver nanoparticles at noncytotoxic doses to HepG2 human hepatoma cells. Environ Sci Technol 43:6046–6051

Kim S, Ryu D-Y (2013) Silver nanoparticle-induced oxidative stress, genotoxicity and apoptosis in cultured cells and animal tissues. J Appl Toxicol 33:78–89

Kim S, Choi JE, Choi J, Chung KH, Park K, Yi J, Ryu DY (2009) Oxidative stress-dependent toxicity of silver nanoparticles in human hepatoma cells. Toxicol In Vitro 23:1076–1084

Kim T-H, Kim M, Park H-S, Shin US, Gong M-S, Kim H-W (2012) Size-dependent cellular toxicity of silver nanoparticles. J Biomed Mater Res A 100A:1033–1043

Laban G, Nies LF, Turco RF, Bickham JW, Sepulveda MS (2010) The effects of silver nanoparticles on fathead minnow (*Pimephales promelas*) embryos. Ecotoxicology 19(1):185–195

Liau SY, Read DC, Pugh WJ, Furr JR, Russell AD (1997) Interaction of silver nitrate with readily identifiable groups: relationship to the antibacterial action of silver ions. Lett Appl Microbiol 25:279–283

Lim D, Roh J-Y, Eom H-J, Choi J-Y, Hyun JW, Choi J (2012) Oxidative stress-related PMK-1 P38 MAPK activation as a mechanism for toxicity of silver nanoparticles to reproduction in the nematode *Caenorhabditis elegans*. Envir Toxicol Chem 31:585–592

Lima R, Seabra AB, Durán N (2012) Silver nanoparticles: a brief review of cytotoxicity and genotoxicity of chemically and biogenically synthesized nanoparticles. J Appl Toxicol 32:867–879

Limbach LK, Wick P, Manser P, Grass RN, Bruinink A, Stark WJ (2007) Exposure of engineered nanoparticles to human lung epithelial cell: influence of chemical composition and catalytic activity on oxidative stress. Environ Sci Technol 41:4158–4163

Liu W, Wu Y, Wang C, Li HC, Wang T, Liao CY, Cui L, Zhou QF, Yan B, Jiang GB (2010) Impact of silver nanoparticles on human cells: effect of particle size. Nanotoxicol 4:319–330

Lowry OH, Rosebrough NJ, Farr AL, Randall RJ (1951) Protein measurement with the Folin phenol reagent. J Biol Chem 193:265–275

Lubick N (2008) Nanosilver toxicity: ions, nanoparticles or both? Environ Sci Technol 42:8617–8676

Miura N, Shinohara Y (2009) Cytotoxic effect and apoptosis induction by silver nanoparticles in HeLa cells. Biochem Biophys Res Commun 390:733–737

Nair PMG, Park SY, Lee SW, Choi J (2010) Differential expression of the ribosomal protein gene, gonadotrophin releasing hormone gene and Balbiani ring protein gene as mechanisms of the toxicity on exposure to silver nanoparticles in fourth instar larvae of the aquatic midge, *Chironomus riparius*. Aquat Toxicol 101:31–37

Navarro E, Piccapietra F, Wagner B, Marconi F, Kaegi R, Odzak N, Sigg L, Behra R (2008) Toxicity of silver nanoparticles to *Chlamydomonas reinhardtii*. Environ Sci Technol 42:8959–8964

Nel AE, Mädler L, Velegol D, Xia T, Hoek EM, Somasundaran P, Klaessig F, Castranova V, Thompson M (2009) Understanding biophysicochemical interactions at the nano-bio interface. Nat Mater 8:543–557

Panda KK, Achary VMM, Krishnaveni R, Padhi BK, Sarangi SN, Sahu SN, Panda BB (2011) In vitro biosynthesis and genotoxicity bioassay of silver nanoparticles using plants. Toxicol In Vitro 25:1097–1105

Park EJ, Yi J, Kim Y, Choi K, Park K (2010) Silver nanoparticles induce cytotoxicity by a Trojan-horse type mechanism. Toxicol In Vitro 24:872–878

Piao MJ, Kanga KA, Leeb IK, Kimb HS, Kimc S, Choid JY, Choie J, Hyuna JW (2011) Silver nanoparticles induce oxidative cell damage in human liver cells through inhibition of reduced glutathione and induction of mitochondria-involved apoptosis. Toxicol Lett 201:92–100

Racker E, Horstmann LL (1967) Partial resolution of the enzymes catalyzing oxidative phosphorylation XIII. Structure and function of submitochondrial particles completely resolved with respect to coupling factor F_1. J Biol Chem 242:2547–2551

Rahman MF, Wang J, Patterson TA, Saini UT, Robinson BL, Newport GD, Murdock RC, Schlager JJ, Hussain SM, Ali SF (2009) Expression of genes related to oxidative stress in the mouse brain after exposure to silver-25 nanoparticles. Toxicol Lett 187:15–21

Raveendran P, Fu J, Wallen SL (2003) Completely "green" synthesis and stabilization of metal nanoparticles. J Am Chem Soc 125:13940–13941

Samberg ME, Oldenburg SJ, Nancy A, Monteiro-Riviere NA (2010) Evaluation of silver nanoparticle toxicity in skin in vivo and keratinocytes in vitro. Environ Health Perspect 118:407–413

Sharma VK, Yngard RA, Lin Y (2009) Silver nanoparticles: green synthesis and their antimicrobial activities. Adv Colloid Interface Sci 145:83–96

Tang J, Xiong L, Wang S, Wang J, Liu L, Li J, Yuan F, Xi T (2009) Distribution, translocation and accumulation of silver nanoparticles in rats. J Nanosci Nanotechnol 9:4924–4932

Teodoro JS, Simões AM, Duarte FV, Rolo AP, Murdoch RC, Hussain SM, Palmeira CM (2011) Assessment of the toxicity of silver nanoparticles in vitro: a mitochondrial perspective. Toxicol In Vitro 25:664–670

Turrens JF (2003) Mitochondrial formation of reactive oxygen species. J Physiol 552:335–344

Ulrich F (1964) The inhibition of mitochondrial adenosine triphosphatase 2. The effects of amino acids and sugars. Arch Biochem Biophys 104(2):248–256

Vasileva P, Donkova B, Karadjova I, Dushkin C (2011) Synthesis of starch-stabilized silver nanoparticles and their application as a surface plasmon resonance-based sensor of hydrogen peroxide. Colloids Surf A 382:203–210

Völker C, Oetken M, Oehlmann J (2013) The biological effects and possible modes of action of nanosilver. Rev Environ Contamin Toxicol 223:81–106

Woodrow Wilson International Center for Scholars (2013) A nanotechnology consumer products inventory. http://www.nanotechproject.org/cpi/about/analysis/,fig. 5

Xiu Z-M, Ma J, Alvarez PJJ (2011) Differential effect of common ligands and molecular oxygen on antimicrobial activity of silver nanoparticles versus silver ions. Environ Sci Technol 45:9003–9008

Yang X, Gondikas AP, Marinakos SM, Auffan M, Liu J, Hsu-Kim H, Meyer JN (2012) Mechanism of silver nanoparticle toxicity is dependent on dissolved silver and surface coating in *Caenorhabditis elegans*. Environ Sci Technol 46:1119–1127

Zeiri I, Bronk BV, Shabtai Y, Eichler J, Efrima S (2004) Surface-enhanced Raman spectroscopy as a tool for probing specific biochemical components in bacteria. Appl Spectrosc 58:33–40